Antiferromagnetic Stabilization in the Ti_8O_{12} Cluster

Xiaohu Yu,* Artem R. Oganov, Ivan A. Popov, Guangrui Qian, and Alexander I. Boldyrev

Abstract: *Using the evolutionary algorithm USPEX and DFT + U calculations, we predicted a high-symmetry geometric structure of the bare Ti_8O_{12} cluster composed of 8 Ti atoms forming a cube, in which O atoms are at midpoints of all of its edges, in excellent agreement with experimental results. Using natural bond orbital analysis, adaptive natural density partitioning algorithm, electron localization function, and partial charge plots, we find the origin of the particular stability of bare Ti_8O_{12} cluster: unique chemical bonding where eight electrons of Ti atoms interacting with each other in antiferromagnetic fashion to lower the total energy of the system. The bare Ti_8O_{12} is thus an unusual molecule stabilized by d-orbital antiferromagnetic coupling.*

The photoactivity of TiO_2[1] is one of the most attractive properties for technologies making use of titanium oxide, which include photoelectrochemical splitting of water to hydrogen,[2] oxidation photocatalysis of organic molecules,[3] photovoltaic devices,[4] and superhydrophilicity.[5] Titanium oxide clusters and their derivatives have also attracted great attention owing to their remarkable properties.[6] X-ray diffraction studies show that titanium oxychloride [Ti_8O_{12}-$(H_2O)_{24}$]Cl_8·HCl·$7H_2O$ has a cubic titanium octamer linked to chloride ions and water molecules by a complex network of hydrogen bonds.[7] Titanium oxychloride is useful as a semi-conductor element of a photovoltaic cell or as a photocatalyst in air or water purification treatments.[8] Furthermore, single crystals of titanium oxychloride can be synthesized by gentle hydrolysis of a commercial $TiOCl_2$ solution, and hydrolysis of the titanium oxychloride can be used for synthesis of various TiO_2 materials.[9] Theoretically, the $Ti_8O_{12}H_8$ cluster can be used as an ideal model to study transformation of methanol to formaldehyde.[10] The natural question is: what is the origin of stability of the bare Ti_8O_{12} cluster? Usually, the geometric structure and particularly favorable chemical bonding patterns are associated with the stability of such clusters. There are many reports on unusual chemical bonding modes in stable transition-metal oxide clusters,[11] for example, $(Mo_3O_9)^{2-}$ and $(W_3O_9)^{2-}$ with d-orbital σ aromaticity.[12] Unique π- and δ-aromaticity in the transition-metal oxide cluster $(Ta_3O_3)^-$ is also known.[13] Very recently, d-orbital spherical σ-aromaticity in a stable Ce_6O_8 cluster was found by Yu et al.[14] Herein we report an interesting and unexpected chemical bonding mode in a bare Ti_8O_{12} cluster exhibiting d-orbital antiferromagnetic character, which is contributing to the high stability of the bare cluster.

Extensive searches for global minima of all Ti_8O_n ($n = 1$–18) clusters were performed at the spin-polarized DFT + U level of theory. The predicted global energy minimum of the Ti_8O_{12} cluster has titanium atoms in the corner of the Ti_8 cube and oxygen atoms near midpoints of its edges, which agrees well with experiment.[7] The Ti–Ti, O–O, and Ti–O distances are 3.18, 3.22, and 1.86 Å, respectively. The structures and relative total energies of the ground electronic state and low-lying isomers of Ti_8O_{12} are shown in Supporting Information, Figure S1.

First, we analyzed the stability of Ti_8O_n ($n = 0$–18) clusters using ab initio thermodynamics, with the Gibbs free energy defined as:[15]

$$\Delta G_f(T,p_{O_2}) = F_{Ti_8O_n}(T) - F_{Ti_8}(T) - n\mu_O(T,p_{O_2}) \tag{1}$$

where $F_{Ti_8O_n}(T)$ and $F_{Ti_8}(T)$ are the Helmholtz free energy of the Ti_8O_n and the pristine Ti_8 cluster (at their ground state with respect to geometry and spin), respectively, and $\mu_O(T,p_{O_2})$ is the chemical potential of oxygen. There are twelve stable clusters: Ti_8, Ti_8O_1, Ti_8O_2, Ti_8O_3, Ti_8O_5, Ti_8O_8, Ti_8O_{10}, Ti_8O_{12}, Ti_8O_{13}, Ti_8O_{14}, Ti_8O_{16}, and Ti_8O_{17}, as shown in Figure 1a. We can recast Figure 1a in another insightful form, as shown in the phase diagram (Figure 1b). In equilibrium with molecular O_2 gas, $\mu_O(T,p_{O_2})$ is expressed as:

$$\mu_O(T,p_{O_2}) = \tfrac{1}{2}[E_{O_2} + \mu_{O_2}(T,p^0) + k_B T \ln(p/p^0)] \tag{2}$$

where p^0, k_B, and p are the standard atmospheric pressure, Boltzmann constant, and oxygen partial pressure, respectively. E_{O_2} was obtained from a spin-polarized calculation. The $\mu_{O_2}(T,p^0)$ term includes vibrational, rotational, and magnetic contributions for O_2 gas, and was taken from thermodynamic tables.[16] $k_B T \ln(p/p^0)$ is the contribution of temperature and O_2 partial pressure to the oxygen chemical potential.

[*] Dr. X. Yu, Prof. Dr. A. R. Oganov
Department of Problems of Physics and Energetics
Moscow Institute of Physics and Technology
9 Institutskiy Land, Dolgoprudny city (Russia)
E-mail: yuxiaohu950203@126.com

Prof. Dr. A. R. Oganov
Skolkovo Institute of Science and Technology
Skolkovo Innovation Center, 5 Nobel St., 143026 (Russia)

Prof. Dr. A. R. Oganov, Dr. G. Qian
Department of Geosciences and Center for Materials by Design
Stony Brook University, Stony Brook
New York 11794 (USA)

Prof. Dr. A. R. Oganov
International Center for Materials Discovery
School of Materials Science, Northwestern Polytechnical University
Xi'an 720072 (China)

Dr. I. A. Popov, Prof. Dr. A. I. Boldyrev
Department of Chemistry and Biochemistry
Utah State University, Logan, UT 84322 (USA)

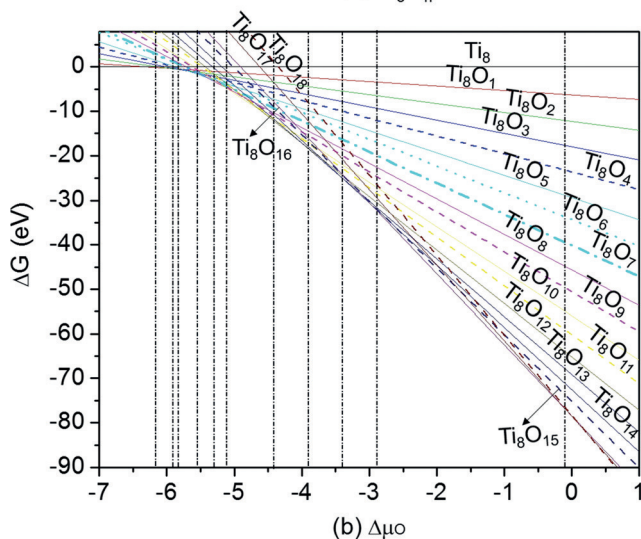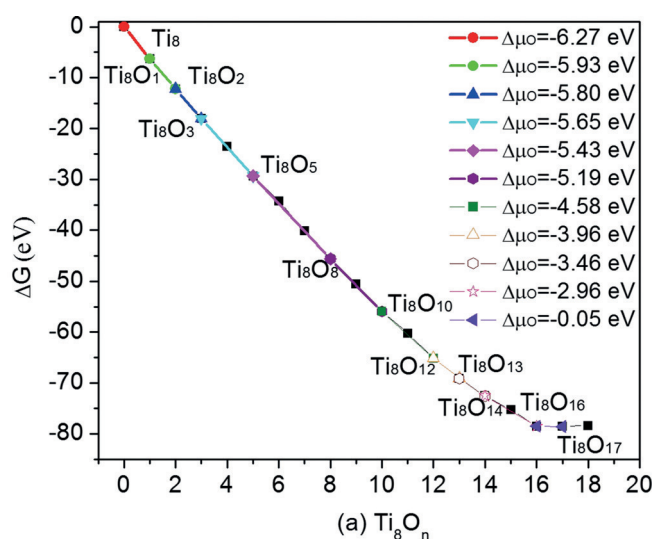Supporting information for this article is available on the WWW under http://dx.doi.org/10.1002/anie.201508439.
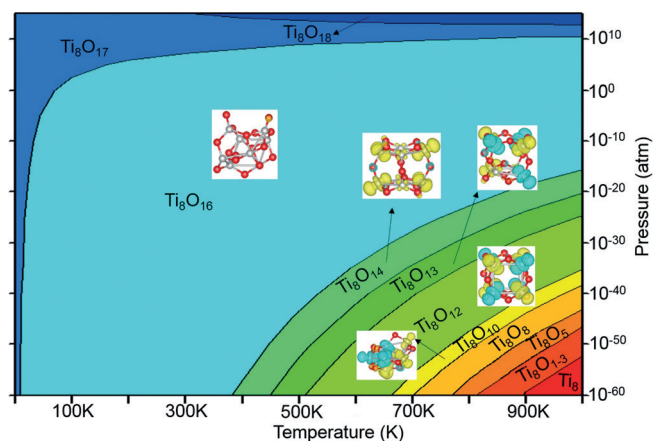
Figure 2. Phase diagram of Ti_8O_n in oxygen atmosphere. The spin distribution (spin up: yellow; spin down: light blue) of the corresponding clusters is shown in the phase diagram.
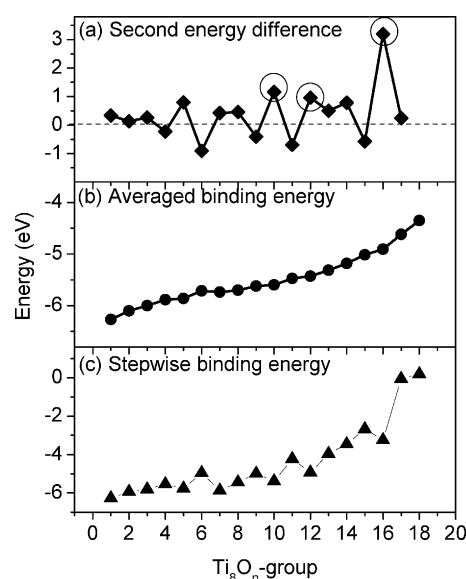

Figure 1. Phase diagram of Ti_8O_n ($n=1–18$) clusters: stability of different clusters as a function of a) chemical composition and b) oxygen chemical potential.

Figure 3. Second energy difference, averaged and stepwise binding energies for global minima Ti_8O_n ($n=1–18$) clusters.

The phase diagram as a function of temperature and partial oxygen pressure is shown in Figure 2; it is clear that Ti_8O_{12} has a wide stability field. Spin density distribution for stable Ti_8O_n ($n=10, 12, 13, 14, 16$) clusters is also shown in Figure 2. The ground state of Ti_8O_{16} cluster is singlet, Ti_8O_{14} is quintet, and Ti_8O_{12} and Ti_8O_{13} clusters are both singlets in antiferromagnetic state.

Then, the second energy difference was used to determine stable clusters of Ti_8O_n; it is defined as:

$$\Delta^2 E = 2E(Ti_8O_n) - E(Ti_8O_{n-1}) - E(Ti_8O_{n+1}) \qquad (3)$$

where $E(Ti_8O_n)$ is the energy of Ti_8O_n cluster. The peaks of second energy difference (Figure 3) correspond to the magic clusters: Ti_8O_{10}, Ti_8O_{12}, Ti_8O_{16}.

The total oxygen binding energy is defined as:

$$\Delta E_n = E(Ti_8O_{12}) - E(Ti_8) - \tfrac{1}{2} n E(O_2) \qquad (4)$$

and the stepwise oxygen binding energy is then

$$\Delta\Delta = \Delta E_n - \Delta E_{n-1} \qquad (5)$$

and the averaged oxygen binding energy is $\Delta E = \Delta E_n/n$. From the stepwise oxygen binding energy (Figure 3), we see that the binding of up to sixteen oxygen atoms on the Ti_8 cluster is particularly favorable thermodynamically, and the averaged oxygen binding energy shows that binding of all eighteen oxygen atoms to the Ti_8 cluster is still thermodynamically feasible.

The stability of Ti_8O_{12} and Ti_8O_{16} is due to closed electronic shell, but Ti_8O_{12} (on which we focus here) also has a highly symmetric atomic structure (O_h symmetry), in contrast to all other Ti_8O_n ($n=1–18$) clusters with lower point group symmetries (Supporting Information, Figure S2). Ti_8O_{12} complexes play an important role in crystallization of

bulk TiO_2.[9,17] There are many experimental reports on the synthesis of Ti_8O_{12} complexes and a series of nano titanium oxides using a Ti_8O_{12} complex.[17,18]

Counting valence electrons, 8 titanium atoms give a total of $8 \times 4 = 32$ electrons for bonding and 12 oxygen atoms can have in total $12 \times 2 \, (O^{2-}) = 24$ electrons. Hence, the formal charge on Ti is assumed to be $+3$. On balance, there are $32 - 24 = 8$ electrons responsible for the direct Ti−Ti bonding. Understanding where these remaining 8 electrons localize is very important for understanding the extra stability of Ti_8O_{12} cluster.

The electron localization function (ELF)[19] proved to be a useful tool for studying chemical bonding in clusters and molecules. It is interesting to find that there is a localization of electron density on faces of Ti_8O_{12} cluster (Supporting Information, Figure S3). This is reminiscent of the newly predicted polyzinc compound containing $[Zn^I_8(HL)_4(L)_8]^{12-}$ (L = tetrazoledianion) cluster core,[20] which is stable and also features a maximum of ELF in faces of Zn_8 cube.

(a) HOMO (isosurface: 0.001 e/Å³)

(b) HOMO-1 (isosurface: 0.0005 e/Å³)

Figure 5. Partial charge images of Ti_8O_{12} cluster: a) HOMO and b) HOMO−1.
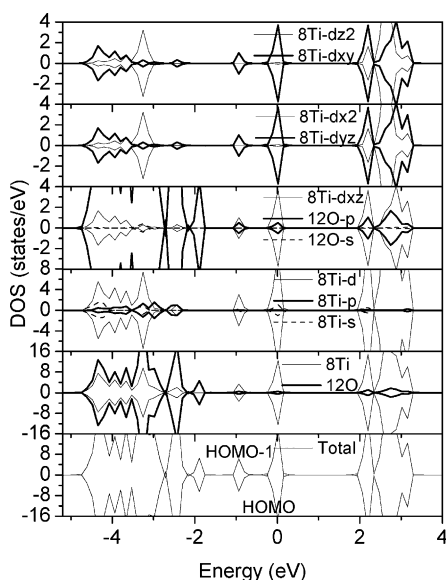

Figure 4. Total and projected densities of states (DOS) of the Ti_8O_{12} cluster.

Figure 4 shows total and projected densities of states (DOS) of the Ti_8O_{12} cluster. From DOS, we can clearly see that the Ti 4s, 3d, 3p hybridize and form bonds with oxygen atoms. Molecular orbitals in the range of −5 to −2 eV are made of strongly hybridized Ti d, Ti p, and Ti s, with O p orbitals forming strongly bonding molecular orbitals. Most interesting bonding molecular orbitals (HOMO−1 state) with energies in the range from −1.2 to −0.8 eV are mainly composed by Ti d_{xy}, d_{yz}, d_{xz}, with a small contribution from O p orbitals. The other interesting molecular orbitals (HOMO state) with energies in the range from −0.3 to 0.3 eV are mainly composed by Ti d_{xy}, d_{yz}, d_{xz}, and a little O p, Ti s, Ti d_{z^2}. The energies in the range from 1.8 to 2.2 eV correspond to antibonding state, which is mainly composed of
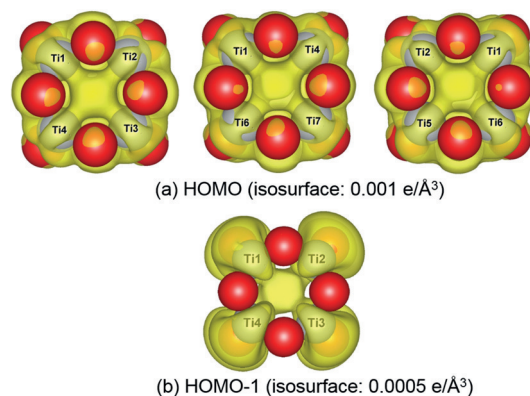
five d orbitals of 8 Ti atoms and a small admixture of oxygen orbitals.

Figure 5 shows partial charge images of the Ti_8O_{12} cluster. From both HOMO and HOMO−1 (Figure 5), the electron density is concentrated inside the Ti_8 fragment (also see the Supporting Information, Figure S4). To get more insight into the electronic structure of the Ti_8O_{12} cluster, we used the natural bond orbital (NBO) as well as its extension, adaptive natural density partitioning analysis (AdNDP) to further interpret the results described above. Previously, AdNDP results have been shown to be insensitive to the level of theory or basis set used.[21] While NBO allows determination of Lewis elements of localized bonding, such as 1c-2e bonds (lone pairs) and 2c-2e bonds (classical two-center two-electron bonds), AdNDP enables delocalized bonding (*nc*-2e bonds, $n > 2$) to be also found. In total, there are 52 valence electron pairs in the cubic Ti_8O_{12} cluster. Similar to the case of highly symmetric Ce_6O_8 cluster,[14] where the localization of two d electrons inside the Ce_6 fragment was found to be responsible for the stability of the cluster, one can assume that eight d electrons coming from eight Ti atoms may also lead to d orbital cubic σ aromaticity according to the $6n + 2$ or $2(n+1)^2$ electron counting rule.[21] Indeed, NBO and AdNDP analyses at the DFT level of theory of a hypothetical non-magnetic Ti_8O_{12} (where all its electrons are paired) show formation of four 8c-2e σ bonds (Supporting Information, Figure S5), responsible for the d-orbital σ aromaticity, akin to the case of Ce_6O_8.[14] However, according to the global minimum search, cubic Ti_8O_{12} is antiferromagnetic in its ground electronic state. Thus, ideally, there should be four unpaired α- and four unpaired β-electrons coming from 8 Ti atoms. Indeed, the complete active space self-consistent field (CASSCF) calculations showed a very strong multiconfigurational nature of the wavefunction (the first leading coefficient is about 0.3) and confirmed the antiferromagnetic character of the cluster (Supporting Information, Table S1). Thus, the natural question is: what causes stabilization of the cluster? In fact, according to the DFT + U calculations, the antiferromagnetic state of the global minimum structure of Ti_8O_{12} is 0.74 eV lower in energy than the ferromagnetic state, while CASSCF calculations show an even greater value of 1.60 eV. We further performed AdNDP analyses of the antiferromag-

netic Ti_8O_{12} using the CASSCF wavefunction to understand how the chemical bonding picture is changed compared to the non-magnetic case. Of note, s-type and p-type lone pairs on oxygen atoms as well as all the 2c-2e Ti−O σ bonds were found to be exactly the same as for the non-magnetic cluster with just slight differences in the occupation number (ON) values. However, the remaining eight electrons were found to localize in accordance with the one-electron symbolic density matrix coefficients for the corresponding orbitals: $a_{1g}^{1.53} t_{1u}^{3.42} t_{2g}^{2.55} a_{2u}^{0.49}$, where a_{1g} and t_{1u} orbitals are bonding, and a_{2u} and t_{2g} are their respective antibonding counterparts. In fact, the totally symmetric 8c-2e σ bond (Supporting Information, Figure S5g) originating from the bonding HOMO−1 (a_{1g}) orbital was found to have lower ON value of 1.53 |e| instead of 1.89 |e|. Noteworthy, three 8c-2e σ bonds (Supporting Information, Figure S5d–f) originating from the triply degenerate HOMO t_{1u} orbital have appreciably lower ON values: 1.14 |e| instead of 1.87 |e|. Thus, one can conclude that there is indeed a certain stabilization coming from some d-AO overlap of 8 Ti electrons, but it cannot be called aromatic as in the case of the hypothetical non-magnetic structure with four bonding orbitals, each occupied by about 2 electrons. Indeed, the geometric factor plays an important role: 8 Ti atoms separated from each other by 12 O atoms are forced to adopt an antiferromagnetic configuration to maximize d-orbital interactions through superexchange, thus lowering the total energy of the system. It should also be pointed out that, primarily, system stabilization is achieved via the strong ionic interactions between Ti^{3+} and O^{2-}. Although common in the solid state, antiferromagnetism in a small cluster is found here for the first time.

In conclusion, using evolutionary structure prediction code USPEX and DFT+U calculations, we found a highly symmetric and stable transition metal oxide cluster Ti_8O_{12}. The phase diagram as a function of temperature and partial oxygen pressure indicates a wide stability field of the Ti_8O_{12} cluster. From the analysis of its electron localization function and electronic structure of Ti_8O_{12}, we found that neutral Ti_8O_{12} cluster is stabilized due to the strong ionic Ti−O bonding and d-orbital antiferromagnetic coupling. The peculiar chemical bonding is likely to make this cluster and its derivatives very interesting for catalysis. We hope that this work will inspire experimental realization of transition metal and lanthanide oxides clusters exhibiting d-orbital antiferromagnetic stabilization.

Experimental Section

The ab initio evolutionary algorithm USPEX,[22] which has been successfully applied to various materials,[23] was used to look for the stable Ti_8O_n ($n = 1–18$) clusters. More detailed description of these calculations can be found in the Supporting Information. To understand chemical bonding in the Ti_8O_{12} cluster, we have utilized NBO[24] and AdNDP[25] analyses, both at PBE0/LANL2DZ and CASSCF(8,10)/LANL2DZ levels of theory using the geometry obtained from VASP calculations. AdNDP has been shown to be a very effective tool for the description of chemical bonding in various systems: from small clusters (0D)[26] to the chain-like species (1D),[27] various atomic-thin sheets (2D),[28] and hypervalent species.[29]

[1] A. L. Linsebigler, G. Lu, J. T. Yates, *Chem. Rev.* **1995**, *95*, 735–758.
[2] A. Fujishima, K. Honda, *Nature* **1972**, *238*, 37–38.
[3] H. Gerischer, A. Heller, *J. Electrochem. Soc.* **1992**, *139*, 113–118.
[4] X. Chen, L. Liu, P. Y. Yu, S. S. Mao, *Science* **2011**, *331*, 746–750.
[5] M. Takeuchi, K. Sakamoto, G. Martra, S. Coluccia, M. Anpo, *J. Phys. Chem. B* **2005**, *109*, 15422–15428.
[6] H.-J. Zhai, L.-S. Wang, *J. Am. Chem. Soc.* **2007**, *129*, 3022–3026.
[7] M. G. Reichmann, F. J. Hollander, A. T. Bell, *Acta Crystallogr. Sect. C* **1987**, *43*, 1681–1683.
[8] L. Brohan, H. Sutrisno, E. Puzenat, A. Rouet, H. Terrisse, Google Patents, **2010**.
[9] C.-E. Liu, A. Rouet, H. Sutrisno, E. Puzenat, H. Terrisse, L. Brohan, M. Richard-Plouet, *Chem. Mater.* **2008**, *20*, 4739–4748.
[10] A. Goodrow, A. T. Bell, *J. Phys. Chem. C* **2008**, *112*, 13204–13214.
[11] J. M. Mercero, A. I. Boldyrev, G. Merino, J. M. Ugalde, *Chem. Soc. Rev.* **2015**, *44*, 6519–6534.
[12] X. Huang, H.-J. Zhai, B. Kiran, L.-S. Wang, *Angew. Chem. Int. Ed.* **2005**, *44*, 7251–7254; *Angew. Chem.* **2005**, *117*, 7417–7420.
[13] H.-J. Zhai, B. B. Averkiev, D. Y. Zubarev, L.-S. Wang, A. I. Boldyrev, *Angew. Chem. Int. Ed.* **2007**, *46*, 4277–4280; *Angew. Chem.* **2007**, *119*, 4355–4358.
[14] X. Yu, A. R. Oganov, I. A. Popov, A. I. Boldyrev, *J. Comput. Chem.* **2016**, *37*, 103–109.
[15] S. Bhattacharya, S. V. Levchenko, L. M. Ghiringhelli, M. Scheffler, *Phys. Rev. Lett.* **2013**, *111*, 135501.
[16] D. R. Stull, H. Prophet, 2nd ed., DTIC Document, U.S. National Bureau of Standards: U.S. EPO, Washington D.C., **1971**.
[17] V. Jouenne, J.-L. Duvail, L. Brohan, E. Gautron, M. Richard-Plouet, *RSC Adv.* **2015**, *5*, 15118–15125.
[18] Y. Li, Q. Sun, S. Ma, M. Zhang, Q. Liu, L. Dong, *ECS J. Solid State Sci.* **2015**, *4*, Q17–Q20.
[19] B. Silvi, A. Savin, *Nature* **1994**, *371*, 683–686.
[20] P. Cui, H.-S. Hu, B. Zhao, J. T. Miller, P. Cheng, J. Li, *Nat. Commun.* **2015**, *6*, 6331.
[21] A. Hirsch, Z. Chen, H. Jiao, *Angew. Chem. Int. Ed.* **2001**, *40*, 2834–2838; *Angew. Chem.* **2001**, *113*, 2916–2920.
[22] a) A. R. Oganov, C. W. Glass, *J. Chem. Phys.* **2006**, *124*, 244704–244715; b) A. R. Oganov, A. O. Lyakhov, M. Valle, *Acc. Chem. Res.* **2011**, *44*, 227–237.
[23] A. O. Lyakhov, A. R. Oganov, H. T. Stokes, Q. Zhu, *Comput. Phys. Commun.* **2013**, *184*, 1172–1182.
[24] a) A. E. Reed, L. A. Curtiss, F. Weinhold, *Chem. Rev.* **1988**, *88*, 899–926; b) E. D. Glendening, C. R. Landis, F. Weinhold, *Wiley Interdiscip. Rev.: Comput. Mol. Sci.* **2012**, *2*, 1–42.
[25] D. Y. Zubarev, A. I. Boldyrev, *Phys. Chem. Chem. Phys.* **2008**, *10*, 5207–5217.

[26] a) I. A. Popov, W.-L. Li, Z. A. Piazza, A. I. Boldyrev, L.-S. Wang, *J. Phys. Chem. A* **2014**, *118*, 8098 – 8105; b) I. A. Popov, V. F. Popov, K. V. Bozhenko, I. Černušák, A. I. Boldyrev, *J. Chem. Phys.* **2013**, *139*, 114307.

[27] I. A. Popov, B. B. Averkiev, A. A. Starikova, A. I. Boldyrev, R. M. Minyaev, V. I. Minkin, *Angew. Chem. Int. Ed.* **2015**, *54*, 1476 – 1480; *Angew. Chem.* **2015**, *127*, 1496 – 1500.

[28] I. A. Popov, Y. Li, Z. Chen, A. I. Boldyrev, *Phys. Chem. Chem. Phys.* **2013**, *15*, 6842 – 6848.

[29] A. S. Ivanov, I. A. Popov, A. I. Boldyrev, V. V. Zhdankin, *Angew. Chem. Int. Ed.* **2014**, *53*, 9617 – 9621; *Angew. Chem.* **2014**, *126*, 9771 – 9775.